

INTERCOMPARISON OF MONTE CARLO RADIATION TRANSPORT CODES MCNPX, GEANT4, AND FLUKA FOR SIMULATING PROTON RADIOTHERAPY OF THE EYE

RADIATION PROTECTION

KEYWORDS: *ocular proton therapy, Monte Carlo simulations, Monte Carlo dose calculation*

S. D. RANDENIYA* *Rice University, Department of Physics and Astronomy
6500 Main Street, Houston, Texas 77005*

P. J. TADDEI and W. D. NEWHAUSER
*The University of Texas M. D. Anderson Cancer Center
Department of Radiation Physics, Unit 94
1515 Holcombe Boulevard, Houston, Texas 77030*

P. YEPES *Rice University, Department of Physics and Astronomy
6500 Main Street, Houston, Texas 77005*

Received April 30, 2008

Accepted for Publication January 31, 2009

Monte Carlo simulations of an ocular treatment beam-line consisting of a nozzle and a water phantom were carried out using MCNPX, GEANT4, and FLUKA to compare the dosimetric accuracy and the simulation efficiency of the codes. Simulated central axis percent depth-dose profiles and cross-field dose profiles were compared with experimentally measured data for the comparison. Simulation speed was evaluated by comparing the number of proton histories simulated per second using each code. The results indicate that all the Monte Carlo transport codes calculate sufficiently accurate proton dose distributions in the eye and that the FLUKA transport code has the highest simulation efficiency.

I. INTRODUCTION

The Monte Carlo technique has been extensively used to study various problems related to proton radiotherapy. Moreover, it is being considered for treatment planning if the simulation times can be reduced to a manageable level. The objective of this study was to evaluate the dose

*E-mail: kdrandeniya@mdanderson.org, randeniya@rice.edu

accuracy and simulation efficiency of Monte Carlo codes MCNPX, GEANT4, and FLUKA for simulating proton dose distributions in the eye.

II. METHODS AND MATERIALS

II.A. Setup Geometry

The simulation geometry consisted of a nozzle and a water phantom (Fig. 1) in accordance with a proton benchmark problem of the American Nuclear Society^{1,2} (ANS). The components of the nozzle, the materials, and their dimensions are listed in Table I. The range shifter was made of Lexan (C₁₆H₁₄O₃) of density 1.20 g/cm³. The brass was 61.5% copper, 35.2% zinc, and 3.3% lead and had a density of 8.49 g/cm³. Two final collimating aperture designs, circular and hemicircular [half-beam block (HBB)], were used for the simulation.

The mean initial energy E of the proton beam was 159 MeV, with an initial Gaussian energy distribution of 3.33% [$\Delta E/E$, the full-width at half-maximum (FWHM) divided by the mean energy]. Laterally, the spatial distribution of the initial intensity of the beam was approximated using a radially symmetric Gaussian distribution with a FWHM of 5 mm. In the simulations, the proton beam traveled 100 mm in air before entering the nozzle. After exiting the final collimating aperture, it traveled

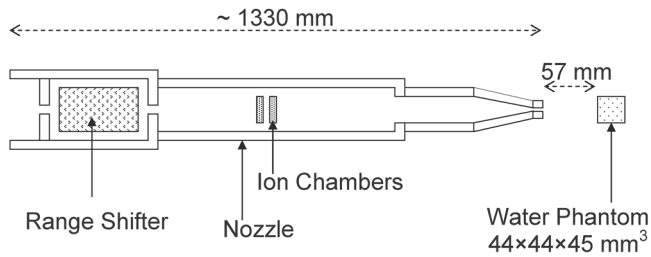


Fig. 1. The geometry of the ocular nozzle and the water phantom used for the simulations in GEANT4 and FLUKA. The components of the nozzle (left to right) are listed in Table I.

TABLE I
Nozzle Components, Materials, and Dimensions
Taken from Ref. 2

Component	Material	Length (mm)	Outer Radius (mm)	Inner Radius (mm)
Range shifter tube	Brass	254	82.6	76.2
First collimator	Brass	10	76.2	6.4
Range shifter	Lexan ^a	62.5	—	—
Second collimator	Brass	10	57.2	12.7
Monitor chamber tube	Brass	681	57.2	51.4
Monitor chamber plates	Aluminum	0.25	25.4	—
Empty tube	Brass	203	44.3	38.5
Tapered tube	Brass	161	44.3	— ^b
Circular aperture	Brass	9.5	20	12
HBB aperture	Brass	9.5	20	13.15

^aThe length of the range shifter is a variable in the simulation that behaves as a combined range and variable degrader.

^bThe inner and outer radii of the snout change as the snout tapers into the final collimating aperture.

57 mm in air before entering the water phantom measuring $44 \times 44 \times 45 \text{ mm}^3$.

The tallies in the phantom recorded the absorbed dose as a function of depth in 180 cylindrical cells, 0.25 mm thick, placed on the beam's central axis. The cross-field absorbed dose profiles were tallied in a linear array of cubical cells placed 0.85 mm apart (center to center) at a depth of 17.5 mm in the water phantom.

The aforementioned geometry was simulated in GEANT4 and FLUKA, and the dosimetric results were compared with ionization chamber (IC) measurements taken at the Northeast Proton Therapy Center (Boston, Massachusetts) and previous simulations using MCNPX, which were included in the ANS benchmark.

II.B. Monte Carlo Codes

II.B.1. MCNPX

The MCNPX data were previously simulated using MCNPX Version 2002a (Ref. 2). The proton transport

physics of this code included energy straggling, multiple Coulomb scattering, elastic and inelastic scattering, and nonelastic nuclear reactions. The low-energy proton transport cutoff was 1 MeV. The particles transported were protons, photons, muons, ^2H , ^3H , ^3He , and alpha particles. More information about this simulation can be found in Ref. 2.

II.B.2. GEANT4

GEANT4 version 4.8.3 (Refs. 3, 4, and 5) was utilized for the simulation with particle transport physics invoked from the standard Hadrontherapy Physics List, which included all the aforementioned electromagnetic and hadronic interactions. The production cutoff of all the particles was set to 100 eV in the simulations. The minimum range of the charged particles in water was set at 20 μm .

II.B.3. FLUKA

The simulation used FLUKA version 2006.3b (Refs. 6, 7, and 8). The particle transport physics in the simulation was set to the FLUKA default settings for hadrontherapy,⁸ which included transport of all the particles described previously plus neutrons. Low-energy transport cutoff of neutrons was set at 19.6 MeV. For the rest of the particles, the transport cutoff was 100 keV, and the fraction of the kinetic energy lost in a step was set at 0.02. Delta ray production threshold was set at 100 keV.

III. RESULTS

III.A. Circular Aperture

For the circular aperture with the aforementioned geometry, the central axis percent depth-dose (PDD) profiles obtained from the simulations along with experimental data and the simulation-to-data ratios are shown in Fig. 2. The maximum dose difference between simulations and IC data at any given depth was $<6\%$ for depths up to 25 mm. In the distal fall-off region (beyond 25 mm depth), the width from the distal 80% dose level to the distal 20% dose level was 3.4, 3.7, and 3.5 mm in the MCNPX, GEANT4, and FLUKA simulations, respectively, as opposed to 3.8 mm in the IC measurements. The Bragg peak fit very well with the IC data (Fig. 2). Hence, all simulations agreed very well with the IC measurements. Statistical uncertainties at the entrance dose, distal 50% dose level, and distal 10% dose level were 0.3, 0.4, and 2.0%, respectively, for 110 million primary particles transported using both FLUKA and GEANT4 simulations. These uncertainties are in good agreement with the reported uncertainties from the MCNPX simulation for 50 million primary protons (0.5, 0.7, and 2.4%, respectively, at the corresponding dose levels).

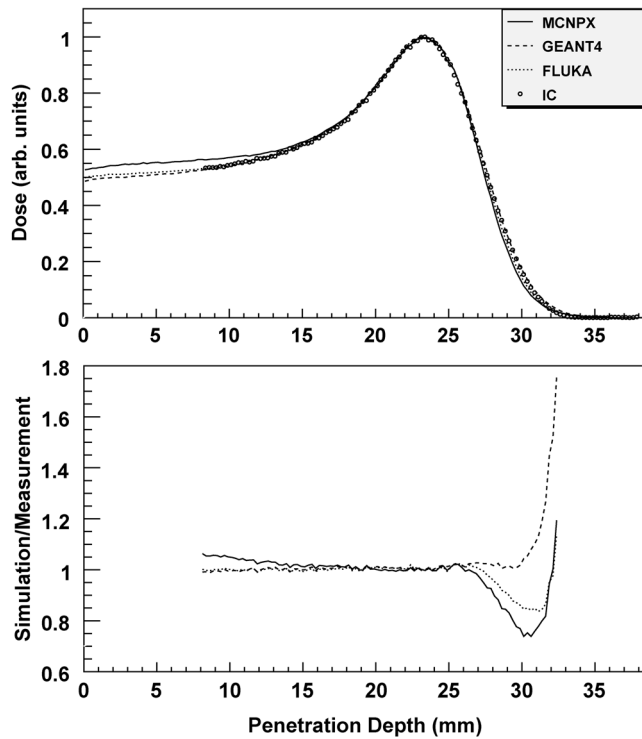


Fig. 2. Central axis PDD profiles obtained from the simulations along with IC data (top) and their ratio with respect to IC data (bottom) for a range setting of 25 mm using the circular aperture.

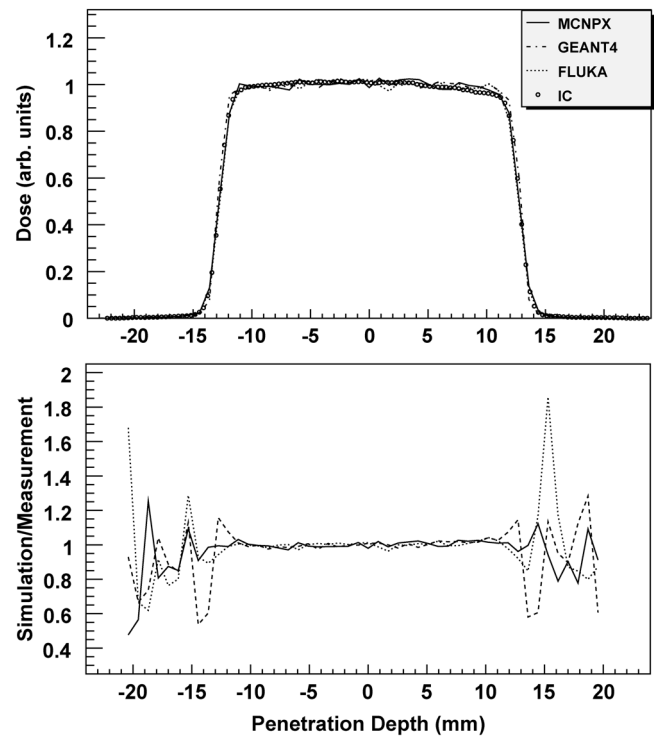


Fig. 3. Cross-field dose profiles obtained from the simulations and the IC data (top) and their ratios (bottom) for the range setting of 25 mm using the circular aperture at a depth of 17.5 mm in the water phantom.

Cross-field profiles obtained from the simulations and their ratios with respect to IC measurements are shown in Fig. 3. The profile ratios from all three simulations had ~2% dose difference between the simulation and IC data in the central region, ~20% difference in the shoulder region, and substantial differences in the penumbral regions. Tables II and III summarize the lateral field width characteristics for the curves shown in Fig. 3. Here, the lateral open-field widths include 90-90%, 80-80%, 50-50%, 20-20%, and 10-10% dose levels and, widths 90-10% and 80-20% dose levels in the penumbral region. The maximum difference in width between simulation and IC data was ~2 mm and occurred at the 90-90% dose level in the GEANT4 simulation. However, the same measurements made using a photographic film reported 1 mm difference for this width for GEANT4. Widths in both FLUKA and MCNPX simulations were at most 1 mm different from IC data and occurred at the same dose level; the film measurements agreed with the simulations within 0.3 mm. Statistical uncertainties were 2, 2, and 6% at the central axis, lateral 50%, and lateral 10% dose levels, respectively, for the 110 million primary protons transported using both FLUKA and GEANT4 simulations. These values agreed very well with the reported uncertainties from the MCNPX simulation, which were 1.25, 1.75, and 5.5%, respectively, at the corre-

TABLE II

Open-Field Widths at Different Dose Levels for the 25-mm Range Setting for the Circular Aperture

Source	Dose Level				
	90-90%	80-80%	50-50%	20-20%	10-10%
IC	22.4 ^a	23.3	25.1	26.9	27.5
Film	23.2	23.9	25.2	26.4	27.2
MCNPX	23.4	24.2	25.6	26.4	27.2
GEANT4	24.2	24.8	25.8	26.6	27.1
FLUKA	23.5	24.2	25.4	26.6	27.2

^aOpen-field widths are in millimeters.

sponding dose levels. Uncertainties of the experimental measurements were not given in Ref. 2.

III.B. Hemicircular Aperture

Tables IV and V summarize preliminary results for the lateral field widths obtained using the GEANT4 and FLUKA simulations along with the reported MCNPX and IC data presented in Ref. 2 for the hemicircular

TABLE III

Penumbra Field Widths (in mm) at Different Dose Levels for the 25-mm Range Setting Using the Circular Aperture

Source	Dose Level at Field Edge (left)		Dose Level at Field Edge (right)	
	80-20%	90-10%	80-20%	90-10%
	IC	1.8 ^a	2.6	1.8
Film	1.3	2.0	1.3	2.0
MCNPX	1.4	2.2	1.4	2.2
GEANT4	0.9	1.4	0.9	1.5
FLUKA	1.3	2.0	1.2	1.8

^aPenumbra field widths are in millimeters.

TABLE IV

Lateral Open-Field Widths for Different Range Settings Using the Hemicircular Aperture

Range (mm)	Source	Dose Level				
		90-90%	80-80%	50-50%	20-20%	10-10%
20	IC	11.8 ^a	12.6	14.3	15.9	16.8
	MCNPX	11.5	12.4	13.9	15.4	16.2
	GEANT4	11.3	11.8	13.0	14.2	15.0
	FLUKA	11.1	11.8	13.1	14.5	15.3
25	IC	11.8	12.7	14.2	15.7	16.4
	MCNPX	12.0	12.7	14.1	15.5	16.2
	GEANT4	11.2	12.2	13.2	14.3	15.4
	FLUKA	11.2	11.9	13.1	14.4	15.3
30	IC	11.9	12.7	14.1	15.5	16.1
	MCNPX	11.9	12.6	14.1	15.4	16.1
	GEANT4	11.7	12.2	13.1	14.4	16.4
	FLUKA	11.4	12.0	13.1	14.5	15.5
35	IC	12.0	12.8	14.1	15.4	16.1
	MCNPX	11.8	12.6	14.0	15.3	15.9
	GEANT4	11.9	12.3	13.2	14.7	16.0
	FLUKA	11.4	12.1	13.2	14.4	16.0
40	IC	12.1	12.8	14.2	15.4	16.1
	MCNPX	12.0	12.7	14.0	15.2	15.8
	GEANT4	11.8	12.2	13.3	14.6	16.7
	FLUKA	11.5	12.0	13.2	14.5	16.3

^aLateral open-field widths are in millimeters.

aperture at five different range settings. The data from the FLUKA simulation agreed with the IC data within 1 mm at the penumbral 90-10% and 80-20% dose levels and at most dose levels of the open-field widths. The maximum difference occurring in lateral field widths was 1.5 mm at the 10-10% dose level for the 20-mm range setting. In the GEANT4 simulation, deviations up to 1.8 mm were observed in the lateral field widths. In the

TABLE V

Penumbra Field Widths for Different Range Settings Using the Hemicircular Aperture

Range (mm)	Source	Dose Level			
		Field Edge		Central Axis	
		80-20%	90-10%	80-20%	90-10%
20	IC	1.7 ^a	2.6	1.6	2.3
	MCNPX	1.6	2.4	1.5	2.3
	GEANT4	1.2	2.0	1.2	1.7
	FLUKA	1.4	2.3	1.3	1.9
25	IC	1.5	2.3	1.4	2.1
	MCNPX	1.5	2.3	1.4	2.1
	GEANT4	1.1	2.6	1.1	1.5
	FLUKA	1.3	1.8	1.3	1.9
30	IC	1.5	2.2	1.3	2.0
	MCNPX	1.4	2.2	1.3	2.0
	GEANT4	1.2	2.9	1.0	1.5
	FLUKA	1.2	2.3	1.2	1.8
35	IC	1.4	2.1	1.2	1.9
	MCNPX	1.4	2.2	1.3	1.9
	GEANT4	1.4	3.4	1.0	1.3
	FLUKA	1.2	2.8	1.1	1.7
40	IC	1.3	2.1	1.3	1.9
	MCNPX	1.3	2.2	1.2	1.6
	GEANT4	1.3	3.0	1.2	1.7
	FLUKA	1.3	3.0	1.2	1.7

^aPenumbra field widths are in millimeters.

penumbra, deviations up to 1.3 were observed, but most dose levels agreed within 1 mm.

III.C. Simulation Speed

The FLUKA simulation transported ~278 primary protons per second in a 2.2-GHz AMD64 Opteron CPU with parallel processing, while the GEANT4 simulation transported ~20 primary protons per second. The simulation efficiency reported for the MCNPX simulation² was ~50 protons per second in a 1.8-GHz Pentium 4 processor. These simulation efficiencies suggest that FLUKA is a factor of ~4 faster than the MCNPX simulation and factor of 14 faster than the GEANT4 simulation.

IV. CONCLUSIONS

The central axis PDD values from all the Monte Carlo codes of interest differed at most by 6% and typically by 2% from the measured dose distributions in the phantom using the circular aperture; the distal 80 to 20% fall-off widths agreed to within 0.4 mm. The simulated lateral open-field widths agreed within a millimeter with the

film measurements. This analysis thus demonstrated that MCNPX, GEANT4, and FLUKA calculate sufficiently accurate proton dose distributions for the eye and that FLUKA has the highest simulation efficiency.

ACKNOWLEDGMENTS

This work was supported in part by the Gulf Coast Center for Computational Cancer Research under contract CABC-2006-5-PY, the Rice Computational Research Cluster funded by the National Science Foundation under Grant CNS-0421109, and a partnership between the Rice University, Advanced Micro Devices, and Cray, and in part by Northern Illinois University through a subcontract of Department of Defense contract W81XWH-08-1-0205.

REFERENCES

1. W. D. NEWHAUSER, N. KOCK, and U. TITT, "ANS-RT-PROTON-01: Prediction of Absorbed Dose Distributions and Neutron Dose Equivalent Values," American Nuclear Society, 2005; available on the Internet (<http://cmpwg.ans.org/benchmarks.html>).
2. W. D. NEWHAUSER, N. KOCK, S. HUMMEL, M. ZIEGLER, and U. TITT, *Phys. Med. Biol.*, **50**, 5229 (2005).
3. S. AGOSTINELLI et al., "GEANT4—A Simulation Tool Kit," *Nucl. Instrum. Methods Phys. Res. A*, **506**, 250 (2003).
4. J. ALLISON et al., "GEANT4 Developments and Applications," *IEEE Trans. Nucl. Sci.*, **53**, 270 (2006).
5. GEANT4 website, <http://geant4.web.cern.ch/geant4/>.
6. A. FASSO, A. FERRARI, J. RANFT, and P. R. SALA, "FLUKA: A Multi-Particle Transport Code," CERN-2005 10 (2005), INFN/TC_05/11, SLAC-R-773.
7. A. FASSO et al., "The Physics Models of FLUKA: Status and Recent Developments," *Proc. Conf. Computing in High Energy and Nuclear Physics*, La Jolla, California, 2003, paper MOMT005, eConf C0303241 (2003), arXiv:hep-ph/0306267.
8. FLUKA official website, <http://www.fluka.org>.